Oxidation of salicylic acid in water by the O_3 and UV/O_3 processes: removal and reaction byproducts

Chang Jing, Wang Shaopo, Zhang Yaxue, Wang Yibo, Zhang Wenjuan, Lu Jinfeng and Wang Zhe

ABSTRACT

In this study, the removal of salicylic acid (SA) in water by ozone (O_3) and ultraviolet/ozone (UV/O_3) processes was investigated. Results showed that more than 50% of SA (10 mg/L) could be effectively removed after 1 min during these two processes. However, the UV/O_3 process was much more effective than the O_3 process for SA mineralization, and the total organic carbon reduction after 30 min was 69.5% and 28.1%, respectively. In the two processes, the optimum pH value for SA removal was 4.3, while that for SA mineralization was 10.0. Both bicarbonate and dissolved organic carbon significantly inhibited SA removal during the two processes. Eleven oxidation byproducts were detected in O_3 process, but only four byproducts were observed in UV/O_3 process. Three hydroxylation aromatic products were identified as the initial byproducts during SA degradation. Glyoxylic acid monohydrate, glycolic acid, and oxalic acid were accumulated in O_3 process but not observed in UV/O_3 process. Oxalic acid was the only detected small molecular byproduct in UV/O_3 process, and it could be further mineralized, thereby indicating that UV/O_3 had a greater potential for degrading both SA and its reaction byproducts.

Key words | byproduct, degradation pathway, ozone, removal efficiency, salicylic acid, ultraviolet/ozone

Chang Jing
Wang Shaopo
Wang Yibo
Zhang Wenjuan
School of Environmental and Municipal Engineering, Tianjin Key Laboratory of Aquatic Science and Technology,
Tianjin Chengjian University,
Tianjin 300384,
China

Zhang Yaxue
Shenzhen Water Planning and Design Institute Company Limited,
Shenzhen 518000,
China

Lu Jinfeng
College of Environmental Science and Engineering,
NanKai University,
Tianjin 300071,
China

Wang Zhe (corresponding author)
School of Environmental Science and Safety Engineering,
Tianjin University of Technology,
Tianjin 300384,
China
E-mail: *zhewang041@163.com*

INTRODUCTION

Salicylic acid (SA), as an important organic synthetic raw material, is widely used in medicines, pesticides, dyes, rubber, foods and perfumes. In the last decade, owing to its vast usage, SA has become an emerging organic contaminant in the aquatic environment and has been frequently detected in surface water resources and groundwater (Petrie *et al.* 2015).

SA residual in the water environment can cause significant adverse effects on human health, such as central nervous system disorders and blood circulation failure (Chen *et al.* 2019). However, the removal efficiency of SA is limited during conventional water treatment processes. Data obtained from several wastewater treatment works in the UK show that SA removal by the secondary treatment processes is less than 50% (Petrie *et al.* 2015). The conventional drinking water treatment processes, including coagulation/flocculation, sedimentation, and sand filtration, can only degrade a part of SA in raw water (Yang *et al.* 2017). Therefore, advanced technologies are necessary to improve SA removal in water treatment processes, and the application of advanced oxidation processes (AOPs) is viable. AOPs are technologies based on the generation of hydroxyl radicals. The hydroxyl radical (HO•) has a very high oxidation potential of 2.8 V (Legrini *et al.* 1993). They can non-selectively react with various refractory organic pollutants, and usually achieve satisfactory removal and mineralization effects (Miklos *et al.* 2018).

Ozone (O_3) is an oxidant widely used for drinking water treatment because of its oxidation and disinfection potential (Gomes *et al.* 2017). Ozonation is also considered as an attractive option as a tertiary treatment step in wastewater treatment plants to reduce the discharge of micropollutants

doi: 10.2166/wst.2020.155

(Chon *et al.* 2015). O_3 can efficiently remove organic contaminants through selective molecular O_3 reactions and relatively non-selective HO• reactions (Gunten 2003). Because ozonation involves the HO• oxidation pathway, it can be considered an AOP or AOP-like process (Miklos *et al.* 2018). However, during the O_3 process, the mineralization of organic contaminants is generally low and may result in the production of harmful species (Gunten 2003). In order to further improve the performance of ozonation, O_3 can be used in combination with hydrogen peroxide (H_2O_2), catalysts, and ultraviolet (UV) light, thereby forming O_3/H_2O_2, O_3/catalyst, and UV/O_3 AOPs, respectively (Miklos *et al.* 2018). Compared with the O_3 process alone, these combined processes may reduce the O_3 dosage and the yields of harmful species and actively enhance the formation of HO• to promote mineralization (Gomes *et al.* 2017).

To date, SA ozonation has been investigated by several researchers, who have mainly focused on catalytic ozonation, such as O_3/Fe^{2+}, O_3/Mn^{2+} and Fe-Cu@SiO_2/O_3 processes (Parisheva & Nusheva 2007; Gagnon *et al.* 2008; Koricic *et al.* 2016; Chen *et al.* 2019). These authors found that catalytic ozonation is an effective method to remove SA from water. In contrast to individual ozonation, catalytic ozonation has greater potential for SA mineralization, and the mineralization rate possibly depends on the initial pH, O_3 concentration, and type of catalyst (Koricic *et al.* 2016; Chen *et al.* 2019).

Besides catalytic ozonation, the $UV_{254\,nm}/O_3$ process is also considered an attractive water treatment technology. UV and O_3 have been widely used for pretreatment, advanced treatment, and disinfection in water treatment plants. Many studies have demonstrated that the combination of UV and O_3 can significantly enhance the oxidation/mineralization of refractory organic contaminants and disinfection byproduct precursors compared with individual technologies (Legrini *et al.* 1993; Miklos *et al.* 2018; Munir *et al.* 2019). This is mainly because the UV/O_3 process involves complex chemical reactions; thus, organic contaminants and their reaction intermediates/byproducts can be degraded by multiple pathways. The main pathways include radical (HO•) oxidation, direct O_3 oxidation, and direct UV photolysis (Glaze *et al.* 1987; Peyton & Glaze 1988). Moreover, in the UV/O_3 system, HO• generation is complex and mainly results from the following reactions: first, $UV_{254\,nm}$ photolysis of aqueous ozone produces H_2O_2 (Reaction (1)) and then UV photolysis of H_2O_2 generates HO• (Reaction (2)). In addition, the decomposition of O_3 initiated by peroxide and hydroxide ions can also produce HO• (Reactions (3)–(6)) (Staehelin & Hoigne 1982; Peyton & Glaze 1988; Oh *et al.* 2005).

$$O_3 + H_2O + h\nu \rightarrow O_2 + H_2O_2 \quad (1)$$

$$H_2O_2 + h\nu \rightarrow 2HO\bullet \quad (2)$$

$$O_3 + H_2O_2 \rightarrow HO_2^-\bullet + HO\bullet + O_2 \quad k = 1.0 \times 10^{-2}\,M^{-1}\cdot s^{-1} \quad (3)$$

$$H_2O_2 \leftrightarrow HO_2^- + H^+ \quad pK_a = 11.6 \quad (4)$$

$$O_3 + OH^- \rightarrow HO_2^- + O_2 \quad k = 70\,M^{-1}\cdot s^{-1} \quad (5)$$

$$O_3 + HO_2^- \rightarrow O_2^-\bullet + HO\bullet + O_2 \quad k = 5.5 \times 10^6\,M^{-1}\cdot s^{-1} \quad (6)$$

However, studies on SA degradation by the UV/O_3 process are limited. Therefore, it is worth investigating the performance of UV/O_3 in SA degradation, which may provide useful data for the selection and optimization of water treatment methods to achieve complete removal of SA in real water. In this study, the degradation of SA by the UV/O_3 process was investigated, including the efficiency of removal and mineralization; influences of initial pH, bicarbonate (HCO_3^-), and dissolved organic carbon (DOC); oxidation byproducts; and degradation pathways. Experiments on the O_3 process alone for SA degradation were conducted simultaneously, and the results were compared with those obtained by the UV/O_3 process. Based on these results, differences between the UV/O_3 and O_3 processes for SA degradation are discussed.

MATERIALS AND METHODS

Materials

SA (≥99.0%) was purchased from Sigma-Aldrich (USA). A stock solution of SA (500 mg/L) was prepared using ultrapure water (18.2 MΩ·cm, Millipore Corp., USA). All organic solvents were HPLC grade and purchased from Merck (Germany). Sulfuric acid (H_2SO_4), sodium hydroxide (NaOH), sodium thiosulfate ($Na_2S_2O_3$), and sodium bicarbonate ($NaHCO_3$) were analytical grade and purchased from Tianjin Ruimingwei Chemical Industry Co., Ltd (China). Humic acid was purchased from Beijing Huawei Ruike Chemical Co., Ltd (China) and its stock solution was prepared according to the report by Shawwa & Smith (2001). *N*-methyl-*N*-(trimethylsilyl)-2,2,2-trifluoroacetamide

(MSTFA) with 1% trimethylchlorosilane was used for gas chromatography derivatization and purchased from Tianjin Hongfeng Weili Technology Development Co., Ltd (China). All solutions were prepared with ultrapure water.

Experimental procedures

Experiments were conducted in a cylindrical reactor with an inserted quartz glass tube. The volume of the reaction solution was 1 L. A UV lamp (253.7 nm; 9 W; Aqua zonic, China) was turned on to warm up for 30 min before being placed inside the quartz glass tube of the reactor. The UV light intensity in the water was measured by a UV-254 radiometer (LS125-P254-WP, China). It was specifically used for the light intensity measurement of the UVC lamp in water and the probe was waterproof within 1 m depth under water. The probe was inserted into water at different depths to detect the UV light intensity and the average intensity was 2,600 μW/cm^2. O_3 was produced by an O_3 generator (Com-AD-01, Anseros, China) using air as the source gas. O_3 gas was introduced into the reaction system through a bubble diffuser at a flow rate of 0.8 L/min. The equilibrium concentration of O_3 was 2.4 mg/L at 30 min in ultrapure water without UV radiation.

For the UV/O_3 experiment, after adding SA solution with a certain concentration to the reactor, the UV lamp and O_3 gas were simultaneously introduced to the reaction system. The procedures of the O_3-only and UV-only experiments were the same as those of the UV/O_3 experiment, but the UV lamp was turned off in the O_3 experiment and O_3 was not introduced in the UV experiment. The ambient temperature was 20 °C and the initial pH of the reaction solution was not adjusted (4.3 ± 0.1). H_2SO_4 and NaOH were used to adjust the pH of the solution during the pH-influenced experiments, and $NaHCO_3$ was added to the system to investigate the effects of HCO_3^-. The appropriate volume of humic acid stock solution was added to the reaction solution to investigate the effect of initial DOC concentration. At given time intervals, a certain volume of sample was withdrawn from the reactor and used for analysis. The residual O_3 in the sample was quenched by the addition of an aliquot of 0.1 mol/L $Na_2S_2O_3$. Each experiment was repeated three times, and the error bar in the figures indicates the standard deviation of the mean.

MSTFA derivatization

Oxidation byproducts containing -OH/-COOH functional groups were derivatized with MSTFA. MSTFA could react with the -COOH and -OH groups, thereby forming trimethylsilyl derivatives (Yu *et al.* 1998). The detailed derivatization steps were as follows: 10 mL of reaction solution was freeze-dried and then 500 μL of dichloromethane and 10 μL of MSTFA were added. After shaking for 1 min, the sample was derivatized for 60 min in a water bath at 60 ± 1 °C. Finally, the sample was removed and prepared for gas chromatography/mass spectrometry (GC/MS) analysis.

Analysis

The SA concentration was detected at 300 nm by a high performance liquid chromatography (HPLC) instrument (Agilent 1100LC, USA) equipped with a UV detector and a ZORBAX SB-C18 column (4.6×150 mm, 5 μm). The mobile phase was water containing 0.1% formic acid (v/v) and acetonitrile with a ratio of 60:40. The detection limit of the method was 10 μg/L.

MSTFA-derivatized compounds were analyzed by gas chromatography with electron ionization mass spectrometry (GC/EI-MS) (GCMS-TQ8040, Shimadzu) with an RTx-5 MS column (Shimadzu). The GC temperature program was as follows: holding at an initial temperature of 60 °C for 1 min, increasing to 300 °C at rate of 10 °C/min, and holding for 2 min. The source temperature was maintained at 230 °C. The identification of MSTFA-derivatized compounds was conducted according to Yu *et al.* (1998).

Total organic carbon (TOC) was determined by a Shimadzu TOC-VCPH analyzer. The O_3 concentration was detected via the indigo method reported by Bader & Hoigné (1981) using disulfonate rather than trisulfonate.

RESULTS AND DISCUSSION

Removal and mineralization of SA

SA oxidation by the O_3 process in pure water is shown in Figure 1. It was observed that when the initial concentrations of SA were 5 mg/L and 10 mg/L, more than 50% of SA could be removed after 1 min and the SA concentration reduced below the detection limit after 3 min and 4 min, respectively. But for 20 mg/L of SA, the removal efficiency decreased under the same condition, and 86.2% of SA was removed at 10 min. Batch ozonation experiments conducted by Hu *et al.* (2016) also indicated that SA can be removed by ozonation within a short contact time. Thus, ozonation was an effective method to remove SA from water.

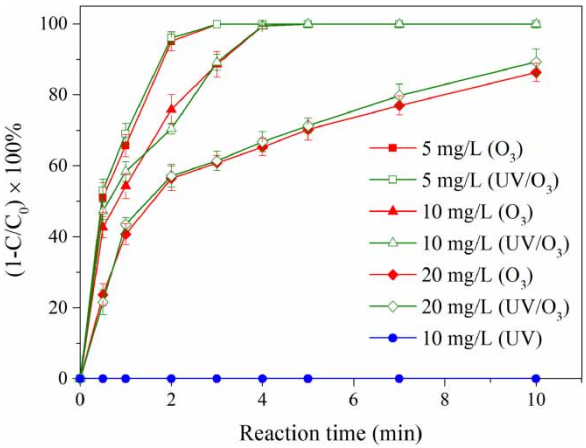

Figure 1 | Removal of SA at different initial concentrations (5 mg/L, 10 mg/L and 20 mg/L). Conditions: pH = 4.3, T = 20 °C, UV intensity = 2,600 μW/cm^2.

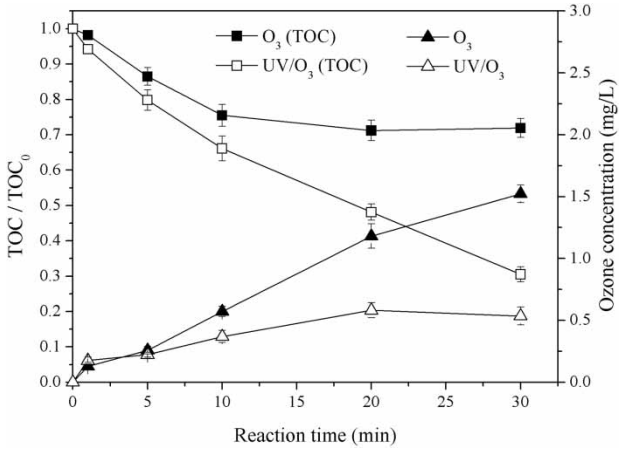

Figure 2 | Mineralization of SA and ozone concentration during O_3 and UV/O_3 processes. Conditions: $[SA]_0$ = 10 mg/L, pH = 4.3, T = 20 °C, UV intensity = 2,600 μW/cm^2.

The trends of SA (5 mg/L, 10 mg/L and 20 mg/L) removal by the UV/O_3 process were also studied, as illustrated in Figure 1. The results were similar between UV/O_3 and O_3 processes when the same initial SA concentration was used. For example, for 10 mg/L of SA, the maximum difference of SA removal efficiency was 5.4% in the two processes, at 2 min of the reaction time. UV photolysis of SA was also investigated because it is an important reaction process involved in the UV/O_3 reaction. However, SA (10 mg/L) degradation was not observed in the UV process, as shown in Figure 1. Feng *et al.* (2004) also found that the degradation of SA (100 mg/L) was negligible under irradiation of two 8 W UVC lamps. UV-spectra of SA exhibited that SA had absorption peaks at 215 nm, 238 nm and 304 nm, respectively (Tian *et al.* 2009). This indicated that direct photolysis could not lead to significant degradation of SA when the UV lamp at 253.7 nm was used because of the weak absorbance of SA at this wavelength.

Even if SA was effectively removed by the O_3 process and UV/O_3 process, there were clear differences in SA mineralization between the two processes. As shown in Figure 2, during the O_3 process, only 24% of mineralization was reached at 10 min, and then the TOC concentration changed insignificantly. Instead, the UV/O_3 process was able to mineralize SA continuously, and 70% of TOC could be reduced at 30 min. The aqueous O_3 concentrations in the reaction systems were also detected simultaneously. It was found that the O_3 concentration differed clearly in the two processes (Figure 2). In the O_3 process, the O_3 concentration significantly increased from 0.13 mg/L at 1 min to 1.52 mg/L at 30 min, while in the UV/O_3 process it increased from 0.18 mg/L at 1 min to 0.58 mg/L at 20 min, and then changed insignificantly.

In the UV/O_3 process, UV irradiation provides an additional energy that promotes O_3 decomposition to generate more HO• (Reactions (1) and (2)) (Miklos *et al.* 2018). This is helpful for the mineralization of reaction intermediates and byproducts because HO• has less discrimination regarding the type of functional group it will attack (Gunten 2003). Moreover, the reaction intermediates/byproducts of SA resulting from HO• and O_3 oxidation can also be further degraded by UV photolysis, which does not exist in the O_3 process. All the above reactions can enhance the mineralization of SA in the UV/O_3 process.

Investigation of influencing parameters

The ozonation reaction and decomposition are affected by water quality, and main parameters are alkalinity, pH, and natural organic matter (NOM) (Lado Ribeiro *et al.* 2019). In this study, the effects of the initial solution HCO_3^-, pH, and NOM on the degradation of SA by O_3 and UV/O_3 processes were investigated.

Effect of HCO_3^-

Alkalinity in natural water is mainly caused by HCO_3^-, carbonate (CO_3^{2-}), and hydroxide (OH^-), and HCO_3^- is the main form in water. However, HCO_3^- is an inhibitor of O_3 decomposition and a typical HO• scavenger, as shown in Reaction (7) (He *et al.* 2012). The effect of HCO_3^- on SA removal was studied, as shown in Figure 3. When HCO_3^- (20 mM) was added to the reaction solution, it exhibited

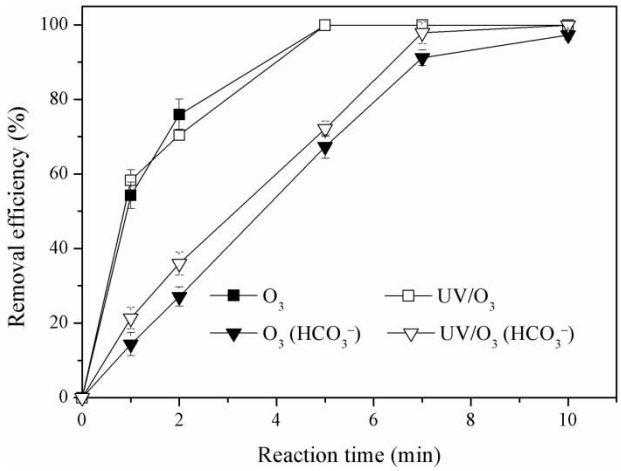

Figure 3 | Effect of HCO_3^- on SA degradation during O_3 and UV/O_3 processes. Conditions: $[SA]_0 = 10$ mg/L, $[HCO_3^-]_0 = 20$ mM, pH = 4.3, T = 20 °C, UV intensity = 2,600 μW/cm^2.

significant inhibition of SA removal in both the O_3 and UV/O_3 processes before 5 min, but the inhibition was insignificant after 7 min. This indicated that in both the O_3 and UV/O_3 systems, HO• played an important role in removing SA, and HCO_3^- was an important factor that could influence the performances of these two processes. According to Reaction (7), HCO_3^- can scavenge HO• with the formation of CO_3^-•, which is more selective than HO• as oxidant (Lado Ribeiro *et al.* 2019). Thus, the removal of SA was affected to a certain extent. But, in the two processes the inhibition of HCO_3^- gradually weakened as the reaction proceeded. This was probably because, in the presence of high HCO_3^- concentrations, the decomposition of ozone was inhibited due to the HCO_3^- scavenging of HO• (Lado Ribeiro *et al.* 2019), and the direct O_3 oxidation of SA could be enhanced. In addition, results in Figure 3 showed that the inhibition of SA removal by HCO_3^- in the O_3 process was greater than that in the UV/O_3 process, which proved that the O_3 process was susceptible to the effect of HCO_3^- in this study.

$$HO\bullet + HCO_3^- \rightarrow H_2O + CO_3^-\bullet \quad k = 8.5\times10^6\,M^{-1}\cdot s^{-1} \qquad (7)$$

Effect of initial solution pH

The effect of initial solution pH (2.0, 4.3, and 10.0) on SA removal by the O_3 process and UV/O_3 process is shown in Figure 4(a). In these two processes, the removal efficiency was the highest at pH 4.3 while it was the lowest at pH 2.0. Moreover, there were no clear differences between the O_3 and UV/O_3 processes for removing SA under the conditions of pH 4.3 and 10.0. However, at pH 2.0, O_3 removed SA more effectively than UV/O_3 after 1 min of reaction.

Further study showed that the effect of initial solution pH on SA mineralization differed significantly from that on SA removal. As shown in Figure 4(b), in the O_3 process, with the increase in pH from 2.0 to 10.0, the mineralization of SA increased from 18% to 37% at 10 min. This indicated that a significant improvement in SA mineralization was obtained by increasing the pH value, which was consistent with the results observed by Parisheva & Nusheva (2007). Meanwhile, in the UV/O_3 process, SA mineralization was also significantly promoted by the increase in pH from 2.0

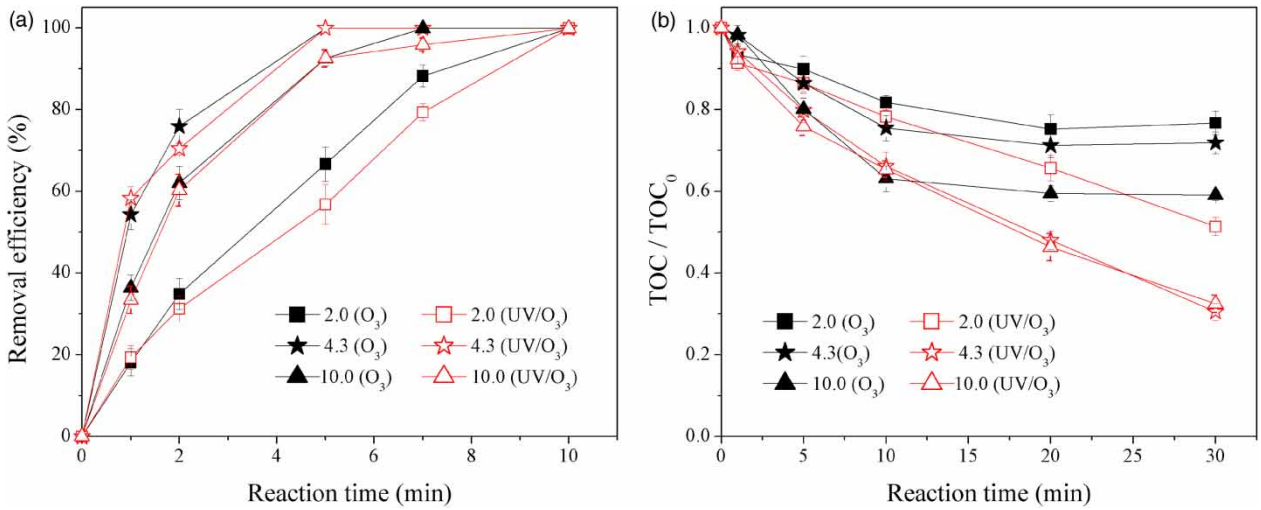

Figure 4 | Effect of initial solution pH on SA removal (a) and mineralization (b) during O_3 and UV/O_3 processes. Conditions: $[SA]_0 = 10$ mg/L, T = 20 °C, UV intensity = 2,600 μW/cm^2.

to 4.3, but not further improved by the increase in pH to 10.0.

It was observed that alkaline conditions (pH 10.0) were more helpful for SA mineralization than acidic conditions (pH 2.0) in both the O_3 and UV/O_3 processes. This was mainly attributed to the influence of solution pH on the stability of dissolved O_3 molecules. According to Reactions (3)–(6), in both the O_3 and UV/O_3 processes, an increase in pH accelerated the decomposition of O_3 and the production of HO•, which promoted the mineralization of SA. However, in the UV/O_3 process, there were not obvious differences in SA mineralization when the pH value was 4.3 and 10.0, which differed from that observed in the O_3 process (Figure 4(b)). Compared with pH 4.3, pH 10.0 resulted in a significant increase of HO^- concentration, which accelerated the decomposition of O_3 to HO•. However, it also significantly reduced the amount of available O_3 for UV photolysis to form H_2O_2, which was also a precursor for HO• formation (Reactions (1) and (2)) (Ratpukdi *et al.* 2010). In addition, as mineralization of SA increased, HCO_3^-/CO_3^{2-} gradually formed in water because of the continuous production of carbon dioxide, and their scavenging effects on HO• became clearer (Reactions (7) and (8)). The effect of HO• scavenging by HCO_3^-/CO_3^{2-} species was related to the value of pH (Ratpukdi *et al.* 2010). At higher pH, CO_3^{2-} concentration increased, and CO_3^{2-} ($k = 3.9 \times 10^8\ M^{-1}{\cdot}s^{-1}$) was more effective in scavenging HO• compared to HCO_3^- ($k = 8.5 \times 10^6\ M^{-1}{\cdot}s^{-1}$) (He *et al.* 2012). Therefore, at pH 10.0, the scavenging of HO• was more significant than that at pH 4.3. It was possible that for these reasons, in the UV/O_3 process, the mineralization of SA at pH 4.3 and 10.0 differed insignificantly.

$$HO\bullet + CO_3^{2-} \rightarrow CO_3^-\bullet + OH^- \quad k = 3.9 \times 10^8\ M^{-1}{\cdot}s^{-1} \qquad (8)$$

Effect of DOC

In natural water, humic substances are important organic constituents of NOM, and humic acid is a principal component of humic substances (Lado Ribeiro *et al.* 2019). In this study, humic acid, as a representative of NOM, was added to the reaction system, and its concentration was indicated by DOC. The effects of the DOC concentration on SA removal by the O_3 and UV/O_3 processes were investigated, as shown in Figure 5. The results showed that humic acid could clearly inhibit SA removal and the O_3 process was inhibited more significantly than the UV/O_3 process. In

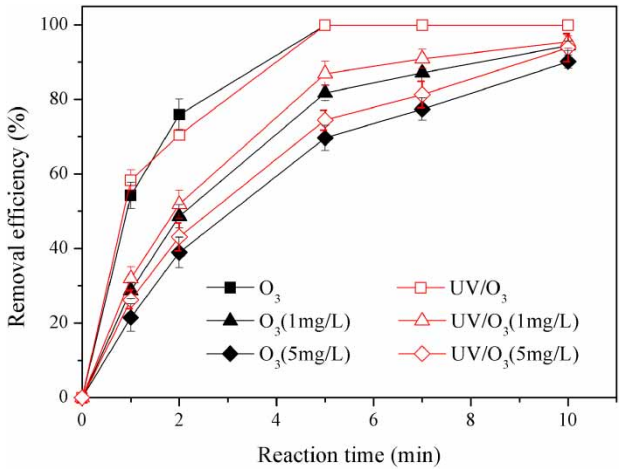

Figure 5 | Effect of DOC on SA degradation during O_3 and UV/O_3 processes. Conditions: $[SA]_0 = 10$ mg/L, pH = 4.3, T = 20 °C, UV intensity = 2,600 μW/cm^2.

the O_3 process with the addition of 1 mg/L and 5 mg/L of humic acid, at 2 min of reaction time, the SA removal efficiency decreased by 27.3% and 36.9%, respectively. Meanwhile, in the UV/O_3 process, the SA removal efficiency decreased by 18.6% and 27.3% respectively. This inhibition possibly resulted from the rich unsaturated structures in humic acid, which were preferentially attacked by HO• and O_3 (Gunten 2003). Therefore, humic acid could compete with SA for the oxidants HO• and O_3 in both the O_3 and UV/O_3 processes.

Oxidation byproducts of SA during the O_3 and UV/O_3 processes

The oxidation byproducts of SA containing -OH/-COOH groups, which were typical byproducts resulting from O_3/HO• oxidation (Gunten 2003), were analyzed by GC/MS. As shown in Table 1, during the O_3 process, 11 byproducts were identified. Three byproducts contained a benzene ring structure – 2,3-dihydroxybenzoic acid, 2,5-dihydroxybenzoic acid, and pyrocatechol – as observed by Hu *et al.* (2016) and Chen *et al.* (2019). The other eight products (1,3-butanediol, butanedioic acid, maleic acid, fumaric acid, 2-hydroxypropanoic acid, glyoxylic acid monohydrate, glycolic acid, and oxalic acid) were chain compounds containing two to four carbons. Among them, maleic acid, fumaric acid, and oxalic acid were also reported by Hu *et al.* (2016) and Chen *et al.* (2019). By comparison, during the UV/O_3 process, only four byproducts

Table 1 | Oxidation byproducts of SA by O_3 and UV/O_3 processes

Oxidation byproducts	Molecular formula	Structural formula	Derivative molecular weight	Useful GC/EI-MS ions (m/z)	O_3	UV/O_3
2,3-Dihydroxybenzoic acid	$C_7H_6O_4$	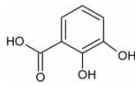	370	73, 193, 265, 355, 370	√	√
2,5-Dihydroxybenzoic acid	$C_7H_6O_4$	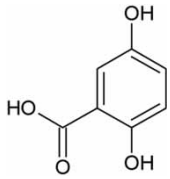	370	73, 147, 223, 297, 355, 370	√	√
Pyrocatechol	$C_6H_6O_2$	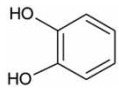	254	73, 239, 254	√	√
1,3-Butanediol	$C_4H_{10}O_2$	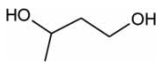	234	73, 103, 117, 129, 147, 191	√	–
Butanedioic acid	$C_4H_6O_4$	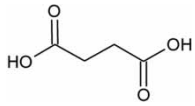	262	73, 129, 147, 247, 262	√	–
Maleic acid	$C_4H_4O_4$	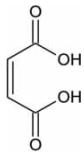	260	73, 133, 147, 245	√	–
Fumaric acid	$C_4H_4O_4$	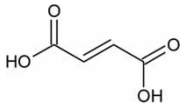	260	73, 143, 147, 245	√	–
2-Hydroxypropanoic acid	$C_3H_6O_3$	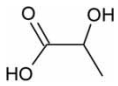	234	73, 117,147, 191, 219	√	–
Glyoxylic acid monohydrate	$C_2H_4O_4$	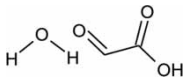	308	73, 147, 191, 221, 265, 293, 308	√	–
Glycolic acid	$C_2H_4O_3$	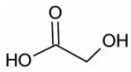	220	73, 133, 147, 161, 177, 205	√	–
Oxalic acid	$C_2H_2O_4$	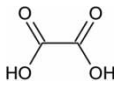	234	73, 133, 147, 175, 190, 219	√	√

(2,3-dihydroxybenzoic acid, 2,5-dihydroxybenzoic acid, pyrocatechol, and oxalic acid) were detected.

Moreover, the yields of SA oxidation byproducts at different reaction times during the O_3 and UV/O_3 processes were also monitored, and were indicated by peak areas obtained in GC/MS chromatograms, as illustrated in Figures 6 and 7. In the O_3 process, all the SA oxidation byproducts obtained their highest yields before 5 min, except for oxalic acid (Figure 6). Among these byproducts, 2,3-dihydroxybenzoic acid, 2,5-dihydroxybenzoic acid, and pyrocatechol, whose structures contained a benzene ring, could be detected at 1 min and reached their maximum concentration at 3 min (Figure 6(a)). They were further degraded significantly and could not be detected at 10 min. Moreover, the amount of 2,5-dihydroxybenzoic acid was dominant, which was consistent with the report by Hu *et al.* (2016). In the SA molecular structure, –OH is a strong electron donating group, and –COOH is an

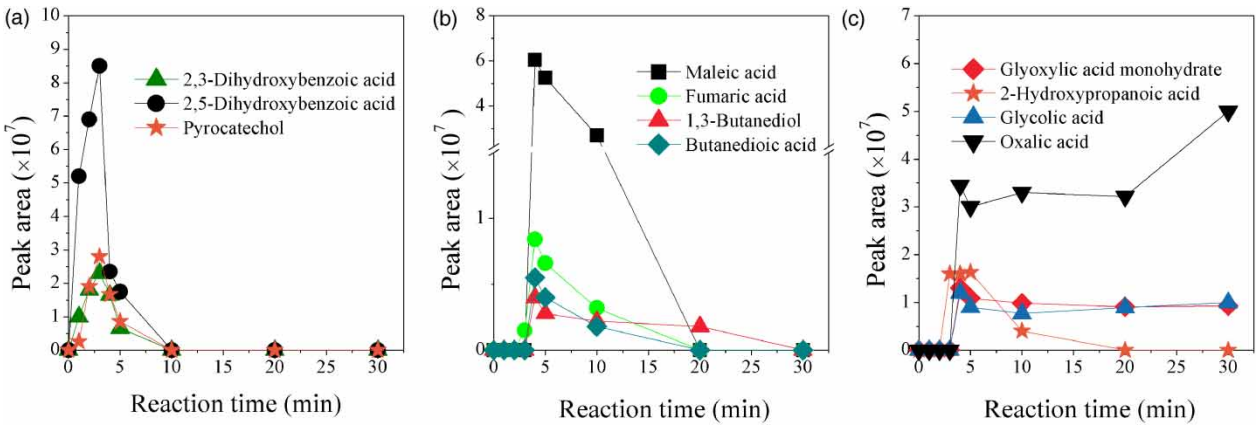

Figure 6 | Oxidation byproducts of SA by O_3 process: byproducts containing benzene ring (a), byproducts containing four carbons (b) and byproducts containing two to three carbons (c). Conditions: $[SA]_0 = 10$ mg/L, pH = 4.3, T = 20 °C.

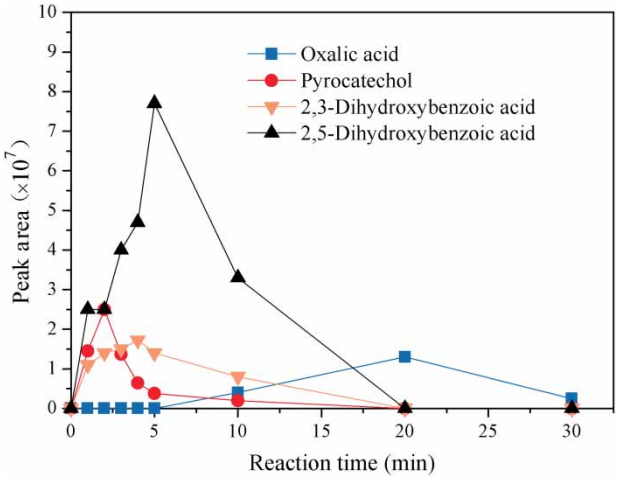

Figure 7 | Oxidation byproducts of SA by UV/O_3 process. Conditions: $[SA]_0 = 10$ mg/L, pH = 4.3, T = 20 °C, UV intensity = 2,600 μW/cm^2.

electron withdrawing group. Effects of both –COOH and –OH make position 5 more electron-rich than position 3 in the benzene ring (Hu *et al.* 2016). Meanwhile, –COOH has the steric hindrance effect at position 3. Therefore, the electrophilic addition of O_3/HO• is prone to occur at position 5 in the benzene ring, forming the prominent byproduct 2,5-dihydroxybenzoic acid. The results in Figure 6(b) show that four chain compounds (1,3-butanediol, butanedioic acid, maleic acid, and fumaric acid), whose structures contained four carbons, could be identified, and their maximum production was at 4 min. As the reaction continued, they were further oxidized and then could not be detected at 30 min. The yield of maleic acid was significantly higher than that of the other three byproducts. At the same time, the other four small molecular compounds containing two to three carbons were also detected before 5 min (Figure 6(c)): 2-hydroxypropanoic acid, glyoxylic acid monohydrate, glycolic acid, and oxalic acid. For 2-hydroxypropanoic acid, its production changed insignificantly during 3–5 min, but was degraded significantly after 5 min and could not be detected at 20 min. The yields of glycolic acid and glyoxylic acid monohydrate reached their maximum at 4 min, declined slightly at 5 min, and were then almost constant. By comparison, oxalic acid had much higher yields. It showed no clear changes during 4–20 min, but increased significantly after 20 min, thereby indicating that there was an accumulation of oxalic acid in the ozonation system, similar to that reported in the literature (Chen *et al.* 2019).

Comparing the results in Figures 6 and 7, it was found that the yields of SA byproducts during the UV/O_3 process differed significantly from those during the O_3 process. In the UV/O_3 process, pyrocatechol, 2,3-dihydroxybenzoic acid, and 2,5-dihydroxybenzoic acid were also identified. Their maximum productions were observed at 2 min, 4 min, and 5 min, respectively. After 20 min, these three byproducts could not be detected. Oxalic acid was the only detected byproduct where the benzene ring was opened, but its production was not significant. Oxalic acid obtained its maximum yield at 20 min and was then further degraded rapidly; this significantly differed from the behavior observed in the O_3 process. Thus, it could be observed that during the UV/O_3 process, the yields of byproducts containing two to four carbons remarkably decreased compared with those during the O_3 process.

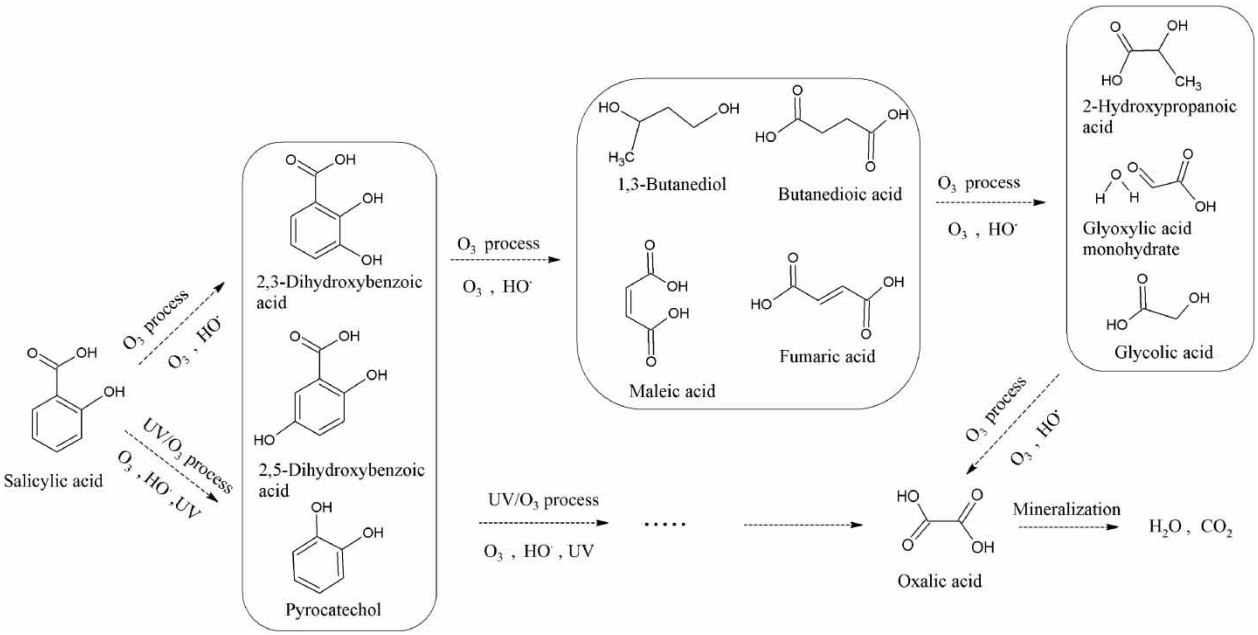

Figure 8 | Possible degradation pathways of SA by O_3 and UV/O_3 processes. Conditions: $[SA]_0 = 10$ mg/L, pH = 4.3, T = 20 °C, UV intensity = 2,600 μW/cm^2.

Degradation pathways of SA by O_3 and UV/O_3 processes

Based on the above SA oxidation byproducts, possible degradation pathways during the two processes are shown in Figure 8. During the O_3 process, under the oxidation of O_3 and HO•, SA was first oxidized to 2,3-dihydroxybenzoic acid, 2,5-dihydroxybenzoic acid, and pyrocatechol, as reported by Hu *et al.* (2016) and Chen *et al.* (2019). During the reaction, their benzene ring structures were opened and then 1,3-butanediol, butanedioic acid, maleic acid, and fumaric acid were formed; their structures contained four carbons. Through further oxidation, smaller molecular byproducts could be produced, namely 2-hydroxypropanoic acid, glyoxylic acid monohydrate, glycolic acid, and oxalic acid.

During the UV/O_3 process, 2,3-dihydroxybenzoic acid, 2,5-dihydroxybenzoic acid, and pyrocatechol were also considered the initial byproducts of SA. However, these byproducts were destroyed more completely. Only one small molecular byproduct, namely oxalic acid, could be detected. It was believed that other small molecular byproducts might have been formed in the reaction, but their yields were too low to be detected. This clear difference between the two processes possibly resulted from the fact that the UV/O_3 process could produce more HO• than the O_3 process and that it additionally involved UV radiation, which could lead to greater mineralization of byproducts.

CONCLUSION

This study investigated the degradation, oxidation byproducts, and the possible degradation pathways of SA by O_3 and UV/O_3 processes. It was apparent that both the O_3 and UV/O_3 processes were effective in the removal of SA from water, but the UV/O_3 process had a significant advantage at mineralizing SA under the same conditions. The influence of the initial pH (2.0, 4.3, and 10.0) showed that the greatest removal of SA was achieved at pH 4.3 in the two processes, but the mineralization of SA could be significantly promoted by increasing the pH, especially in the O_3 process. Moreover, in the UV/O_3 process, the mineralization of SA at pH 4.3 and 10.0 differed insignificantly. The existence of HCO_3^- and DOC could influence the removal of SA in the two processes, and the O_3 process was influenced more significantly. The detection of SA oxidation byproducts showed that under the same conditions, 11 byproducts were identified in the O_3 process, but only 4 byproducts were identified in the UV/O_3 process. Three compounds containing benzene rings (2,3-dihydroxybenzoic acid, 2,5-dihydroxybenzoic acid, and pyrocatechol) were identified as the initial byproducts during the two processes, and they could be further oxidized to small molecular chain compounds. The accumulation of byproducts was observed in the O_3 process, especially that of oxalic acid, which was not observed in the UV/O_3 process. This further proved

that the UV/O_3 process had the advantage of controlling the formation of SA byproducts.

ACKNOWLEDGEMENT

This work was supported by National Natural Science Foundation of China (grant numbers: 51708388; 51608362), and National Science Foundation of Tianjin (grant number: 18JCYBJC23200).

REFERENCES

Bader, H. & Hoigné, J. 1981 Determination of ozone in water by the indigo method. *Water Research* **15** (4), 449–456.

Chen, W., Bao, Y., Li, X., Huang, J., Tang, Y. & Li, L. 2019 Mineralization of salicylic acid via catalytic ozonation with Fe-Cu@SiO_2 core-shell catalyst: a two-stage first order reaction. *Chemosphere* **235**, 470–480.

Chon, K., Salhi, E. & von Gunten, U. 2015 Combination of UV absorbance and electron donating capacity to assess degradation of micropollutants and formation of bromate during ozonation of wastewater effluents. *Water Research* **81**, 388–397.

Feng, J., Hu, X. & Yu, P. L. 2004 Degradation of salicylic acid by photo-assisted Fenton reaction using Fe ions on strongly acidic ion exchange resin as catalyst. *Chemical Engineering Journal* **100** (1), 159–165.

Gagnon, C., Lajeunesse, A., Cejka, P., Gagne, F. & Hausler, R. 2008 Degradation of selected acidic and neutral pharmaceutical products in a primary-treated wastewater by disinfection processes. *Ozone-Science & Engineering* **30** (5), 387–392.

Glaze, W. H., Kang, J. W. & Chapin, D. H. 1987 The chemistry of water-treatment processes involving ozone, hydrogen peroxide and ultraviolet-radiation. *Ozone: Science & Engineering* **9** (4), 335–352.

Gomes, J., Costa, R., Quinta-Ferreira, R. M. & Martins, R. C. 2017 Application of ozonation for pharmaceuticals and personal care products removal from water. *Science of The Total Environment* **586**, 265–283.

Gunten, U. v. 2003 Ozonation of drinking water: part I. Oxidation kinetics and product formation. *Water Research* **37** (7), 1443–1467.

He, X. X., Pelaez, M., Westrick, J. A., O'Shea, K. E., Hiskia, A., Triantis, T., Kaloudis, T., Stefan, M. I., de la Cruz, A. A. & Dionysiou, D. D. 2012 Efficient removal of microcystin-LR by UV-C/H_2O_2 in synthetic and natural water samples. *Water Research* **46** (5), 1501–1510.

Hu, R., Zhang, L. & Hu, J. 2016 Study on the kinetics and transformation products of salicylic acid in water via ozonation. *Chemosphere* **153**, 394–404.

Koricic, K., Kusic, H., Koprivanac, N. & Papic, S. 2016 Mineralization of salicylic acid in water by catalytic ozonation. *Environmental Engineering and Management Journal* **15** (1), 151–166.

Lado Ribeiro, A. R., Moreira, N. F. F., Li Puma, G. & Silva, A. M. T. 2019 Impact of water matrix on the removal of micropollutants by advanced oxidation technologies. *Chemical Engineering Journal* **363**, 155–173.

Legrini, O., Oliveros, E. & Braun, A. M. 1993 Photochemical processes for water-treatment. *Chemical Reviews* **93** (2), 671–698.

Miklos, D. B., Remy, C., Jekel, M., Linden, K. G., Drewes, J. E. & Hübner, U. 2018 Evaluation of advanced oxidation processes for water and wastewater treatment – a critical review. *Water Research* **139**, 118–131.

Munir, H. M. S., Feroze, N., Ikhlaq, A., Kazmi, M., Javed, F. & Mukhtar, H. 2019 Removal of colour and COD from paper and pulp industry wastewater by ozone and combined ozone/UV process. *Desalination and Water Treatment* **137**, 154–161.

Oh, B. S., Kim, K. S., Kang, M. G., Oh, H. J. & Kang, J. W. 2005 Kinetic study and optimum control of the ozone/UV process measuring hydrogen peroxide formed in-situ. *Ozone: Science & Engineering* **27** (6), 421–430.

Parisheva, Z. & Nusheva, L. 2007 Ozonation of aqueous solutions of salicylic acid. *Environment Protection Engineering* **33** (1), 143–150.

Petrie, B., Barden, R. & Kasprzyk-Hordern, B. 2015 A review on emerging contaminants in wastewaters and the environment: current knowledge, understudied areas and recommendations for future monitoring. *Water Research* **72**, 3–27.

Peyton, G. R. & Glaze, W. H. 1988 Destruction of pollutants in water with ozone in combination with ultraviolet-radiation. 3. Photolysis of aqueous ozone. *Environmental Science & Technology* **22** (7), 761–767.

Ratpukdi, T., Siripattanakul, S. & Khan, E. 2010 Mineralization and biodegradability enhancement of natural organic matter by ozone-VUV in comparison with ozone, VUV, ozone-UV, and UV: effects of pH and ozone dose. *Water Research* **44** (11), 3531–3543.

Shawwa, A. R. & Smith, D. W. 2001 Kinetics of microcystin-LR oxidation by ozone. *Ozone: Science & Engineering* **23** (2), 161–170.

Staehelin, J. & Hoigne, J. 1982 Decomposition of ozone in water: rate of initiation by hydroxide ions and hydrogen peroxide. *Environmental Science & Technology* **16** (10), 676–681.

Tian, M., Adams, B., Wen, J., Matthew Asmussen, R. & Chen, A. 2009 Photoelectrochemical oxidation of salicylic acid and salicylaldehyde on titanium dioxide nanotube arrays. *Electrochimica Acta* **54** (14), 3799–3805.

Yang, Y., Ok, Y. S., Kim, K.-H., Kwon, E. E. & Tsang, Y. F. 2017 Occurrences and removal of pharmaceuticals and personal care products (PPCPs) in drinking water and water/sewage treatment plants: a review. *Science of The Total Environment* **596–597**, 303–320.

Yu, J. Z., Flagan, R. C. & Seinfeld, J. H. 1998 Identification of products containing -COOH, -OH, and -C=O in atmospheric oxidation of hydrocarbons. *Environmental Science & Technology* **32** (16), 2357–2370.

First received 20 December 2019; accepted in revised form 25 March 2020. Available online 3 April 2020